Communications

Compression Depth Estimation for CPR Quality Assessment Using DSP on Accelerometer Signals

Sven O. Aase* and Helge Myklebust

***Abstract*—Chest compression is a vital part of cardiopulmonary resuscitation (CPR). This paper demonstrates how the compression depth can be estimated using the principles of inertia navigation. The proposed method uses accelerometer sensors, one placed on the patient's chest, the other beside the patient. The acceleration-to-position conversion is performed using discrete-time digital signal processing (DSP). Instability problems due to integration are combated using a set of boundary conditions. The proposed algorithm is tested on a mannequin in harsh environments, where the patient is exposed to external forces as in a boat or car, as well as improper sensor/patient alignment. The overall performance is an estimation depth error of 4.3 mm in these environments, which is reduced to 1.6 mm in a regular, flat-floor controlled environment.**

***Index Terms*—Accelerometer, compression depth, resuscitation.**

I. Introduction

Chest compression is a vital part of cardio-pulmonary resuscitation (CPR). Over the years, different bodies have issued recommendations where the protocol and performance criteria of CPR are given [1]–[3].

It is a challenge for every rescuer, to both memorize the protocol for resuscitation, and to deliver CPR in compliance with international guidelines. The fact that this is not easy has been demonstrated in many studies and has been discussed in several reviews [4]–[6]. We also know that the significance of early CPR with respect to survival is high [7], [8]. However, not all CPR that is being given is judged to be effective. In one study Wik *et al.* found significantly increased survival in those who received "good" CPR relative to those who received "no good CPR" and no CPR at all [9]. In this case, "good" chest compressions were defined as those giving palpable carotid or femoral pulses.

Our goal for this study was to investigate how well chest compression depth can be estimated using the principle of inertia navigation, which is to calculate change in position based on acceleration. This principle was assessed in 1990 by Gruben *et al.*, but their conclusion was that this was not easily accomplished [10]. Our approach included a selection of instrumentation and signal processing steps aimed to reduce the impact caused by offset drift of the acceleration signal. This was performed on a mannequin. Since resuscitation not always face ideal conditions, we decided to test the method in varying environments, including a boat cruising in a rough sea and a vehicle on a bumpy road. In addition, we studied situations of imperfect positioning of the sensor or patient. A practical, robust, and reliable solution for estimating chest compression depth would enable new kinds of feedback possibilities, not forgetting the value in documenting actually delivered chest compressions. Furthermore, such instrumentation would also enable the use of sophisticated CPR artifact filtering techniques as demonstrated in [11].

Manuscript received September 13, 2000; revised November 20, 2001. *Asterisk indicates corresponding author.*

*S. O. Aase is with Stavanger University College, Department of Electrical and Computer Engineering, P.O. Box 2557 Ullandhaug, N-4004 Stavanger, Norway (e-mail: Sven.O.Aase@tn.his.no).

H. Myklebust is with Laerdal Medical, N-4002 Stavanger, Norway.

Publisher Item Identifier S 0018-9294(02)01740-8.

II. Data Collection and Measurements

A. Mannequin and Sensors

Chest compressions are delivered on a standard Skillmeter mannequin (Laerdal Medical). This mannequin is instrumented with a linear chest compression sensor, formed by an internal pivot acting on a potentiometer. The analog potentiometer signal was made available for our measurement system, and this signal is our reference for the accelerometer based compression depth estimates.

An ADXL202 accelerometer (Analog devices, Cambridge, MA) together with a membrane switch (Keytouch, Horten Norway) comprise the chest compression sensor. The switch is arranged to be activated by the pressure from the rescuer's hands when chest compression begins. A baseplate is secured on top of the mannequin's chest with screws. This baseplate forms a horizontal surface, on which the compression sensor is fixed using adhesive tape.

A second accelerometer, the reference sensor, is put on the floor next to the patient. We use the analog output from each sensor, where the bandwidth is set from direct current to 20 Hz using a resistance-capacitance (*RC*) network. This network also removes anti-aliasing components due to sampling. Even though both accelerometers are two-axis sensors, only the vertical output from each sensor was used.

B. Measurement System

The signals from the two accelerometers, the membrane switch, and the mannequin potentiometer are sampled at 1000 Hz using a PCMCIA data card (DAQ CARD 516, National Instruments) connected to a laptop computer (Compaq Armada 7770). The analog-to-digital conversion gives a resolution of approximately 4.9 mm/s^2 for acceleration and 2.6 μm for vertical displacement of the mannequin chest, without considering noise effects on resolution. For each accelerometer output, the anti-aliasing *RC* filter gives us 35-dB attenuation at 500 Hz.

C. Calibration

The accelerometer sensitivity was set by the difference in output observed for $+g$ and $-g$ input. Applying known displacements for chest compression and observing the corresponding potentiometer outputs gave us the mannequin sensitivity.

D. Recording Sessions

For each session, CPR was performed with two inflations between series of 15 compressions. For the "regular" and "tilt" sessions, we delivered manual chest compressions that included variations in depth, rate and duty cycle. For the "car" and "boat" sessions, we just attempted to comply with the guidelines. At all times, the reference accelerometer was placed on the floor next to the mannequin. The sessions were as follows.

1) *Regular:* Manual CPR was performed with the mannequin lying on the floor. The chest compressions were delivered with variations in duty cycle (20%–50%), with variations in compression rate (60/min–138/min) and with variations in compression depth (2 cm–5 cm). A total of 239 compressions were delivered.
2) *Tilt:* Manual CPR was performed in four cases where either the mannequin was lying on a 10° sloped floor, or where the x-axis of the sensor was mis-aligned by 15° relative to the axis of chest

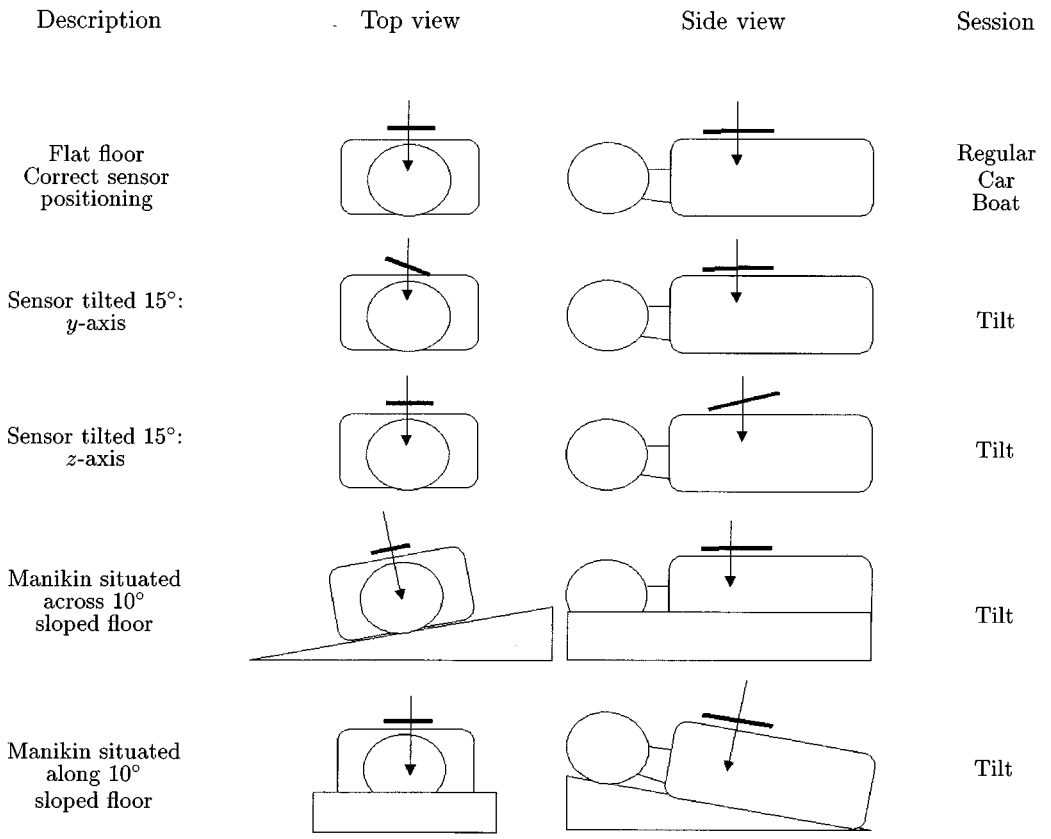

Fig. 1. Overview of mannequin placements in the different sessions.

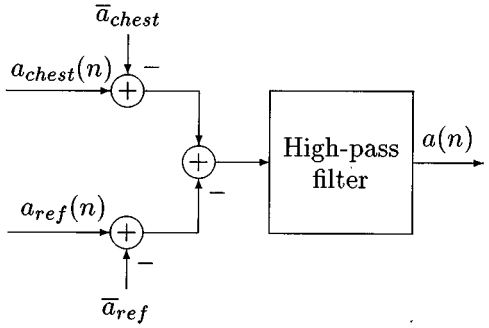

Fig. 2. Preprocessing of acceleration data from two sensors. $a_{\rm ref}(n)$ is the sampled signal from the second accelerometer placed on the floor next to the mannequin.

compression. Chest compressions were delivered with variations in duty cycle (15%–50%), with variations in compression rate (60/min–144/min) and with variations in compression depth (1 cm–5 cm). A total of 336 compressions were delivered.

3) *Car:* Manual CPR was delivered on the mannequin lying on the floor of a moving cargo van (Ford Transit, 1990 model). Our route included several speed reduction bumps, cracks, and holes. For this session, a total of 481 compressions were delivered.
4) *Boat:* Manual CPR was delivered on the mannequin lying on the floor inside an eight ton vessel, cruising at seven knots, taking the seas from all directions. The estimated wave size was 1–1.5 m. For this session, a total of 250 compressions were delivered.

The mannequin and chest sensor orientation in the different sessions are illustrated in Fig. 1.

E. Preprocessing

Acceleration data are collected from two sensors: One placed on the patient's chest, the other beside the patient. The initial data processing is shown in Fig. 2. The high-pass filter is a third-order Butterworth filter with cutoff frequency 0.05 Hz, and is used for removal of any offset components before the integration takes place. In order to minimize transients, the known acceleration offsets are removed by subtracting the constants $\overline{a}_{\rm ref}$ and $\overline{a}_{\rm chest}$ corresponding to $1g$ acceleration on the two sensors. The reference acceleration is then subtracted from the chest acceleration for removal of external acceleration components. In the cases where only the chest sensor data are used, $a_{\rm ref}(n)$ and $\overline{a}_{\rm ref}$ in Fig. 2 are simply set to zero.

III. Discrete-Time Integration

In order to find the chest position $x(t)$, we must integrate the acceleration signal $a(t)$ two times. This operation takes place in the discrete-time domain, referring to signals $a(n)$ and $x(n)$, where n is the discrete index corresponding to time nT.

Starting with the continuous-time formulation the velocity signal $v(t)$ can be written as

$$v(t) = \int_{t_0}^{t} a(\tau)\, d\tau + v(t_0). \tag{1}$$

The integral can be approximated by the trapezoidal formula [12], [13]. Setting $t = nT$ and $t_0 = (n-1)T$, Equation (1) can be converted to the discrete-time domain as

$$v(n) = \frac{T}{2}\left(a(n) + a(n-1)\right) + v(n-1) \tag{2}$$

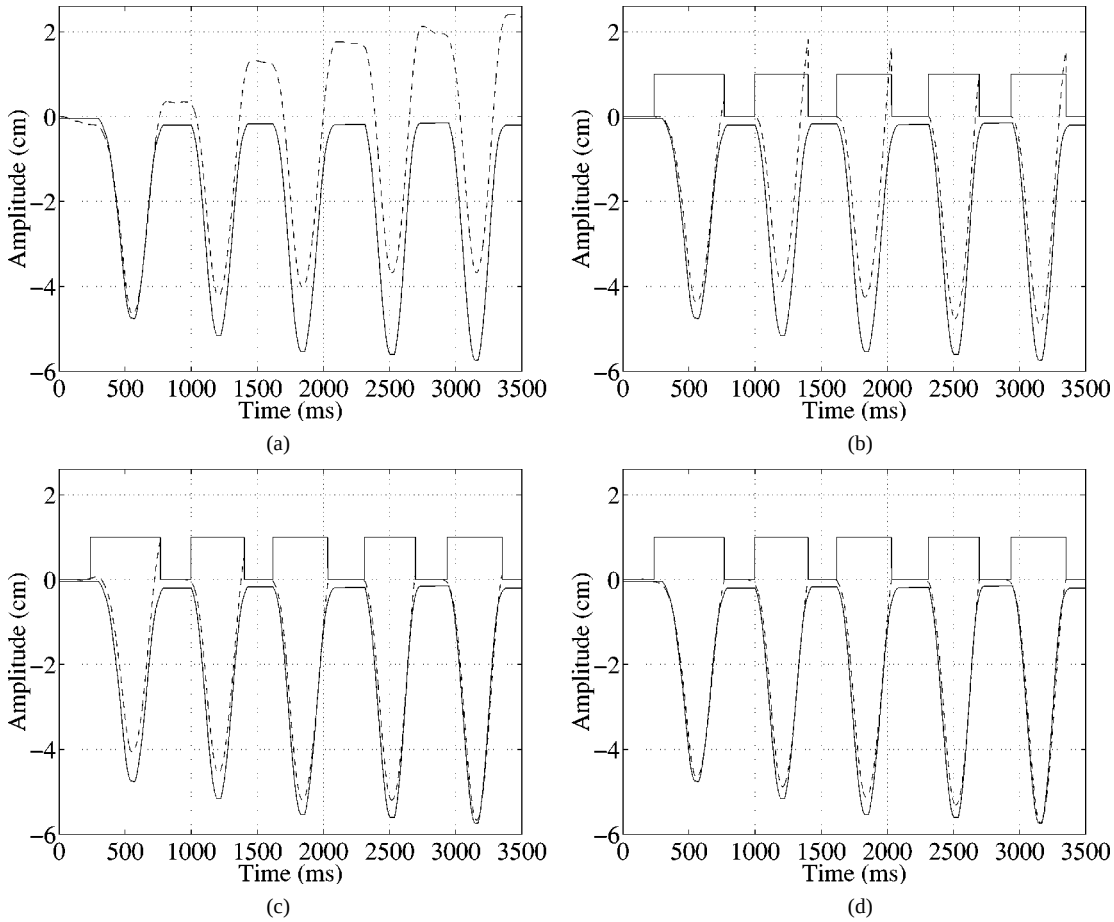

Fig. 3. Comparing estimated position (dashed) with reference position (solid). (a) Straightforward integration. (b) Switched integration. (c) Switched integration advanced by 50 ms. (d) Switched integration advanced by 50 ms using boundary conditions. The switch signal is shown as a solid line in the 0–1 range.

where T is the sample interval accounting for the width of the trapez. Using the Z transform [13] on (2)

$$V(z) = \frac{T}{2}(1 + z^{-1})A(z) + z^{-1}V(z) \tag{3}$$

we obtain the integration transfer function $H(z)$ as

$$H(z) = \frac{V(z)}{A(z)} = \frac{T}{2}\frac{1 + z^{-1}}{1 - z^{-1}}. \tag{4}$$

Using the same derivation for finding $x(n)$ from $v(n)$, the total acceleration-to-position transformation becomes

$$X(z) = (H(z))^2 A(z) = \left(\frac{T}{2}\right)^2 \frac{1 + 2z^{-1} + z^{-2}}{1 - 2z^{-1} + z^{-2}} A(z) \tag{5}$$

which is equivalent to

$$x(n) = 2x(n-1) - x(n-2) + \left(\frac{T}{2}\right)^2 (a(n) + 2a(n-1) + a(n-2)) \tag{6}$$

in the time-domain. This is a second-order difference equation suitable for implementation on a digital signal processor [13]. It should be emphasized that this acceleration-to-position transformation is inherently unstable. When seen as a system function, or filter $G(z) = (H(z))^2$, the filter amplification given a constant input signal is infinite. It follows that special care must be taken in order to eliminate offset components due to noise in the acceleration signal. An example is shown in Fig. 3(a), where the double-integrated acceleration signal is shown and compared with the reference position signal.

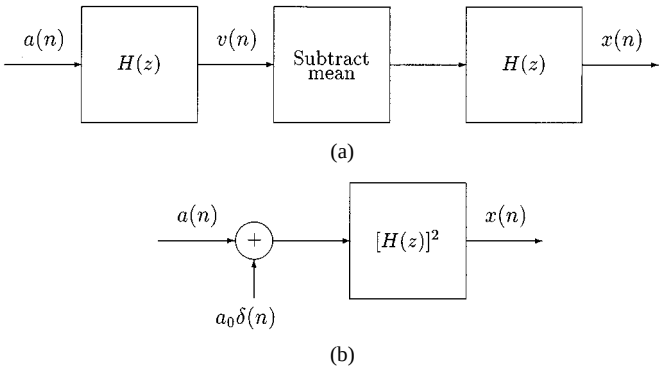

Fig. 4. Alternative means of satisfying the boundary conditions. (a) Velocity mean compensation. (b) Acceleration impulse compensation.

A. Integration Using Reset Mechanism

A practical way of overcoming the stability problem, is to place an on–off switch on the patient's chest, thereby facilitating a simple integrator reset mechanism: Pressing the switch starts the integrator with zero initial conditions and releasing the switch stops the integration process.

This scheme prevents an offset build-up of longer duration than the compress–release cycle. Fig. 3(b) shows the obtained position curve when applied to the same acceleration data as before. Although

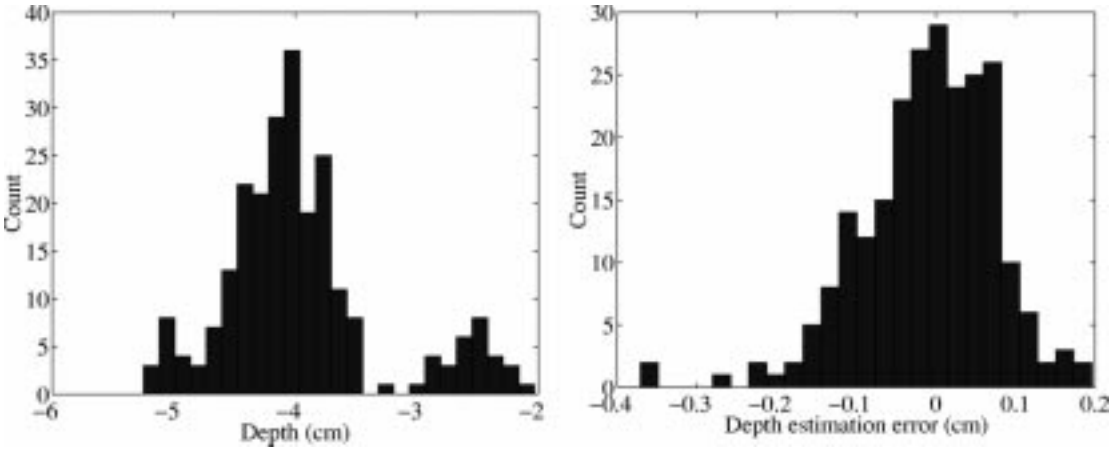

(a) (b)

Fig. 5. Histograms for "Regular" session performance. (a) Compression depth as defined by the reference signal and (b) estimation error.

eliminating the drift problem, the obtained position signal does not follow the reference signal to the maximum compression depth, and rises above zero at the end of the compress–release cycle. Some improvement results if we start the integration process *before* the switch detects the start of a new compress–release cycle. In Fig. 3(c), the integration was started $t_a = 50$ ms in advance of each switch-defined cycle. In practice, some initial sensor acceleration will take place before the switch is set to the "on" position, and this accounts for the improvement.

1) Impulse-Compensated Solution Using Boundary Conditions: In the following, we examine the integration process in one compress–release cycle starting at time $n = 0$ and ending at time $n = P$.

Ignoring for the moment any possible partial deflation of the chest, we assume that the chest position is restored to the same level as that *before* the compression cycle. Denoting this the zero level, we have the following boundary conditions:

$$x(n) = 0, \qquad n < 0 \tag{7}$$

$$a(n) = 0, \qquad n < 0 \tag{8}$$

$$x(P) = 0. \tag{9}$$

From the boundary conditions, we can deduce that the mean value of the velocity signal, computed over the compress–release cycle, must be zero. Knowing that the position is the integrated value of the velocity this follows because the integration process starts [see (7)] and ends [see (9)] with zero value for the position. Incorporating the boundary conditions our system for computing the position signal is as shown in Fig. 4(a).

The addition of a constant (the negative of the velocity mean) *after* a single integration process is equivalent to adding an impulse *prior* to the integration, here at time $n = 0$. This is also shown in Fig. 4(b), where the constant a_0 is chosen such that $x(P) = 0$. This constrained solution has a physical interpretation: When giving chest compression some of the momentum induced by the practitioner's hands creates an acceleration impulse at the onset of each compression. Ideally, using an integration advance of $t_a = 50$ ms as before, this impulse should have been correctly registered by the acceleration sensor. In practice, errors are introduced due to sensor misalignment.

A practical algorithm: The constrained solution for the position signal $x(n)$ is computed on a cycle-by-cycle basis as follows. For each cycle, let $n = 0$ denote the integration start point as defined by the switch and the integration time advance t_a. As before $n = P$ denotes the integration stop point as defined by the switch. Writing the integration input signal as $a(n) + a_0\delta(n)$, the output signal is found as

$$x(n) = x_0(n) + a_0 g(n) \tag{10}$$

where $x_0(n) = (a*g)(n)$ is the unconstrained position signal and $g(n)$ is the unit pulse response of the double-integration system $G(z) = (H(z))^2$. Using (6), it is easily verified that

$$g(n) = \begin{cases} \left(\dfrac{T}{2}\right)^2, & n = 0 \\ T^2 n, & n > 0 \end{cases} \tag{11}$$

which combined with setting $x(P) = 0$ in (10) gives the solution for a_0

$$a_0 = -\frac{x_0(P)}{T^2 P}. \tag{12}$$

Thus, for each compress–release cycle the constrained solution can be found from the following steps.

1) Compute the unconstrained solution $x_0(n)$, $n = 0, \ldots, P$, recursively from (6).
2) Compute the impulse correction weight factor a_0 from (12).
3) Compute the constrained solution $x(n)$, $n = 0, \ldots, P$, from (10).

In contrast to straightforward integration, the proposed scheme introduces a time-delay in the sense that the position signal is not available until the cycle is finished.

Fig. 3(d), shows the obtained result using the proposed scheme for acceleration-to-position conversion. Note that what seems to be an underestimation is in fact correct because the measured reference position signal does not return to the same zero level as that before the start of the compressions. Accordingly, for a compress–release cycle we define the reference compression depth as the difference between the minimum value in the "on" period and the maximum value in the *previous* "off" period. The estimated position signal will, by construction, always return to the zero level, and the compression depth is simply defined as the minimum value in the "on" period.

IV. Evaluation

In the following subsections, we investigate the proposed scheme for acceleration-to-position conversion in very different environments. As

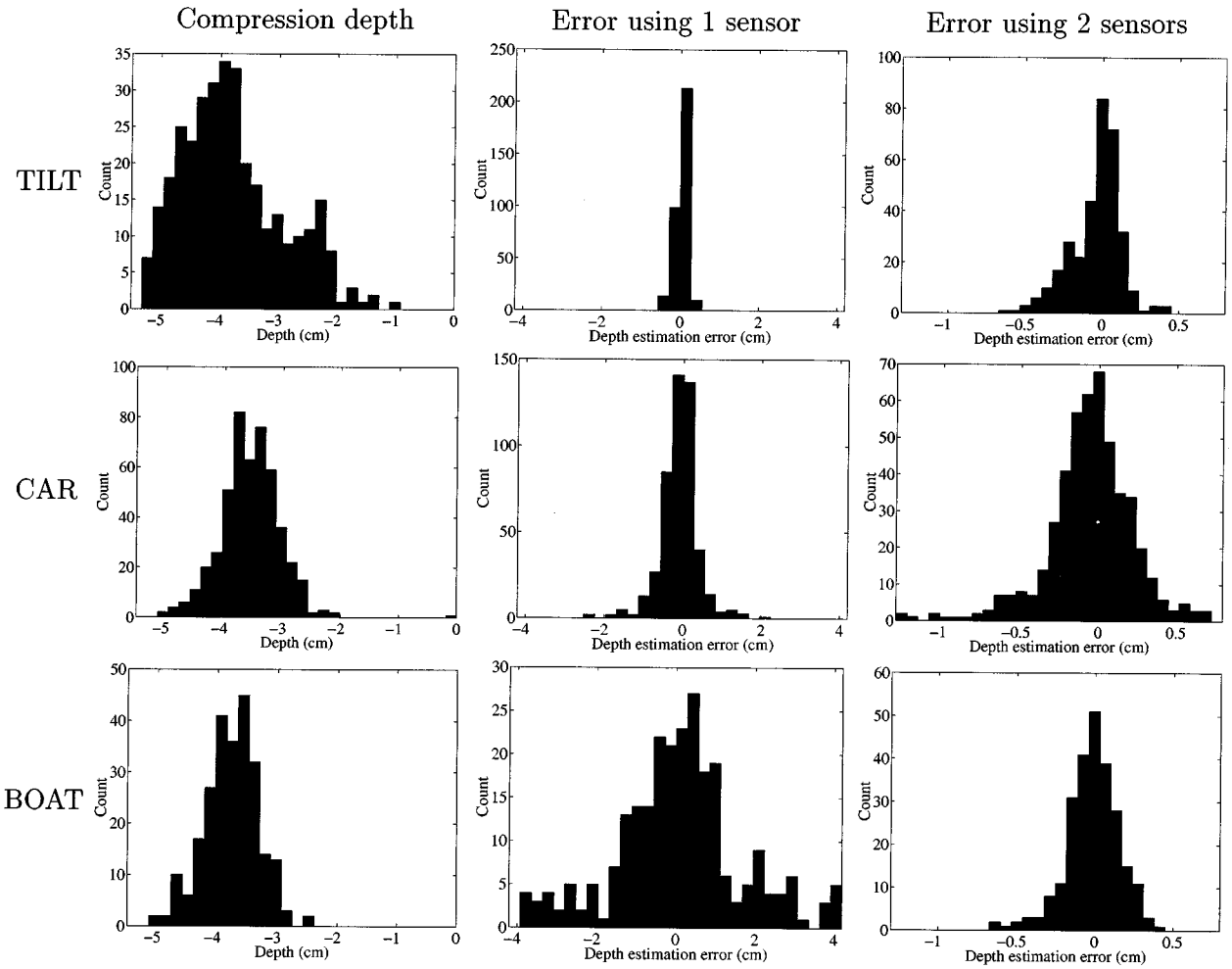

Fig. 6. Performance evaluation in varying environments.

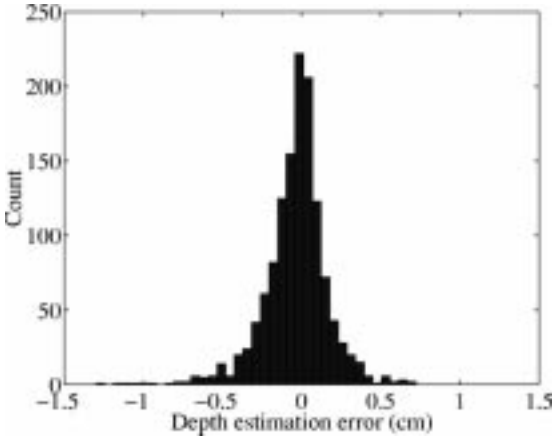

Fig. 7. Overall histogram using two sensors on all four sessions.

described in Section II, we have measured reference position and acceleration signals in four sessions: "Regular," "Tilt," "Car," and "Boat."

A. Histogram for "Regular" Session

Using the acceleration signal from the chest sensor only we obtain an estimate for the position signal. Computing the compression depths as outlined above, we obtain the histograms depicted in Fig. 5.

The error histogram is obtained by subtracting the estimated depth from the reference depth. The proposed scheme detects the compression depth within ± 1.6 mm with 95% confidence when used in this controlled environment.

B. Histograms for Other Sessions

For the sessions "Tilt," "Car," and "Boat," we applied the proposed scheme. For each session, we used the reference- and the estimated position signals to compute histograms for the compression depth and the depth estimation errors using one or two sensors. All histograms are shown in Fig. 6.

In the one-sensor case, the second column of histograms clearly demonstrates how the performance is degraded when the patient is exposed to external accelerating forces: Starting with a narrow histogram for the static "Tilt" session, the "Car" and "Boat" sessions obviously contain increasing amounts of external acceleration, thus rendering wider histograms for the estimation error. Using two sensors, the influence of the external acceleration is diminished and we get similar results for the three sessions, shown in the third column of Fig. 6.

Finally, in Fig. 7 the compression depth estimation error is shown when using two sensors for all four sessions.

C. Overall Evaluation

Table I summarizes our results by showing the 95% confidence of the estimation errors for all sessions. The overall performance using two sensors is ± 4.3 mm within 95% of a total of 1306 compressions.

TABLE I
REGIONS OF 95% CONFIDENCE: FOR EACH HISTOGRAM WE FIND THE POSITIVE VALUE α SUCH THAT 95% OF THE HISTOGRAM AREA LIES BETWEEN $-\alpha$ AND α

Session	1 sensor	2 sensors
Regular	1.6 mm	1.6 mm
Tilt	3.2 mm	3.7 mm
Car	10 mm	6.2 mm
Boat	35 mm	3.6 mm
Overall	–	4.3 mm

V. DISCUSSION AND CONCLUSION

We have evaluated an algorithm for estimation of chest compression depth, where the inputs are signals originating from one accelerometer that follows the movement, one accelerometer that follows the movement of the floor and one switch which is being activated as chest compression begins. Our results indicate that for regular CPR, where the victim is lying flat on the floor, estimated chest compression is within ± 1.6 mm for more than 95% of the compressions. The precision degrades as the conditions for CPR is getting more difficult, like for CPR in a vehicle and in a boat. But this does not imply that the applicability is limited to perfect alignment or flat floor conditions.

The histograms for estimated chest compression depth indicate a Gaussian distribution of the error. Among the contributors to the error is the noise from the accelerometers, which according to the manufacturer's data sheet has a root mean square value six times higher than the quantization step size used in the analog-to-digital converter. When both accelerometers are used to estimate depth, this will increase the error compared with just using one sensor, as seen in Table I for the "Regular" and "Tilt" sessions.

Also contributing to the error is the mannequin reference sensor. Through experiments, we could see that the sensitivity of the position reference sensor in our mannequin varied. Variation was caused by factors like slightly changing supply voltage, different hand position, and the loose fit between mechanical components. Our best estimate is that these factors may cause a sensitivity error of $\pm 3\%$, indicating that a more precise reference for chest compression depth is needed to conclude on performance.

Our method to handle the effect of accelerometer offset and offset drift is based on preprocessing, the activation of the switch, and the integration boundary conditions outlined in Section III-A1.

It is not clear from the literature to which degree manual chest compression depth applied to humans during resuscitation is a variable that plays a significant role with respect to resuscitation outcomes, simply because substantial measurements of this variable are not available. The guidelines for resuscitation will only change with evidence, and we suggest that our method is further validated toward a tool which first of all should be used to assess the clinical importance of manual chest compression variables, including depth, rate, duty cycle, and hands-off intervals.

Limitations of the Study

1) The instrumentation used is a very early prototype, which is designed to attach well to the baseplate of a mannequin's chest. Further improvements are needed to facilitate adhesion and conformity to human chests.
2) Our data is from chest compressions on one mannequin only, and this mannequin does not represent the full variety of chest compliances, compliance variations by time and chest sizes.
3) Our data is from one rescuer only. Even though compressions were delivered with variations in rate, depth, duty cycle, and leaning; further experiments are needed to take individual compression styles into account.
4) Our reference depth data is not from a very precise and stable displacement sensor.
5) Our data are only from experiments where the surface under the mannequin was noncompliant. Degradation of precision due to compliant surfaces like mattresses, beds, and thick clothing must be assessed.

REFERENCES

[1] A. J. Handley, L. B. Becker, M. Allen, A. van Drenth, E. B. Kramer, and W. H. Montgomery, "Single-rescuer adult basic life support," *An Advisory Statement from Basic Life Support Working Group of the International Liason Committee on Resuscitation*, vol. 34, no. 2, pp. 101–108, Apr. 1997.
[2] A. J. Handley, J. Bahr, P. Baskett, L. Bossaert, D. Chamberlain, W. Dick, L. Ekström, R. Juchems, D. Kettler, A. Marsden, O. Moeschler, K. Monsieurs, M. Parr, P. Petit, and A. van Drenth, "The 1998 European resuscitation council guidelines for adult single rescuer basic life support," *Resuscitation*, vol. 37, pp. 67–80, 1998.
[3] R. E. Kerber, *et al.*, "Guidelines for cardiopulmonary resuscitation and emergency cardiac care," *J. Amer. Med. Assoc.*, vol. 268, no. 16, pp. 2171–2302, 1992.
[4] P. Eisenburger and P. Safar, "Life supporting first aid training of the public—Review and recommendations," *Resuscitation*, vol. 41, pp. 3–18, 1999.
[5] W. Kaye and M. E. Mancini, "Teaching adult resuscitation in the United States—Time for a rethink," *Resuscitation*, vol. 37, pp. 177–187, 1998.
[6] M. Liberman, A. Lavoie, D. Mulder, and J. Sampalis, "Cardiopulmonary resuscitation: Errors made by pre-hospital emergency medical personnel," *Resuscitation*, vol. 42, pp. 47–55, 1999.
[7] M. S. Eisenberg, *et al.*, "Cardiac arrest and resuscitation: A tale of 29 cities," *Ann. Emerg. Med.*, vol. 19, no. 2, pp. 179–186, 1990.
[8] L. A. Cobb, *et al.*, "Influence of cardiopulmonary resuscitation prior to defibrillation in patients with out-of-hospital ventricular fibrillation," *J. Amer. Med. Assoc.*, vol. 281, no. 13, pp. 1182–1188, 1999.
[9] L. Wik, P. A. Steen, and N. G. Bircher, "Quality of bystander cardiopulmonary resuscitation influences outcome after prehospital cardiac arrest," *Resuscitation*, vol. 28, pp. 195–203, 1994.
[10] K. G. Gruben, J. Romlein, H. R. Halperin, and J. E. Tsitlik, "System for mechanical measurements during cardiopulmonary resuscitation in humans," *IEEE Trans. Biomed. Eng.*, vol. 37, pp. 204–210, Feb. 1990.
[11] S. O. Aase, T. Eftestøl, J. H. Husøy, K. Sunde, and P. A. Steen, "CPR artefact removal from human ECG using optimal multichannel filtering," *IEEE Trans. Biomed. Eng.*, pp. 1440–1449, Nov. 2000.
[12] P. Kraniauskas, *Transforms in Signals and Systems*. Reading, MA: Addison-Wesley, 1992.
[13] J. G. Proakis and D. M. Manolakis, *Digital Signal Processing: Principles, Algorithms and Applications*, 2nd ed. New York: Macmillan, 1992.